The enhancement of local air pollution by urban CO_2 domes

Mark Z. Jacobson

Department of Civil and Environmental Engineering, Stanford University, Stanford, California 94305-4020, USA; Email: jacobson@stanford.edu; Tel: (650) 723-6836

April 3, 2009

Data suggest that domes of high CO_2 levels form over cities[1-5]. Despite our knowledge of these domes for over a decade[1], no study has contemplated their effects on local temperature or water vapor or the resulting feedback to air pollution and health. In fact, all air pollution regulations worldwide assume arbitrarily that such domes have no local health impact[6] and carbon policy proposals, such as "cap and trade" implicitly assume that CO_2 impacts are the same regardless of where emissions occur. Here, it is found by cause and effect that local CO_2 emissions indeed increase local ozone, particulate matter, and mortality. As such, reducing locally-emitted CO_2 will reduce local air pollution mortality even if CO_2 in adjacent regions is not controlled. This result contradicts the basis for all air pollution regulations worldwide, none of which considers controlling local CO_2 based on its local health impacts. It also suggests that implementation of a "cap and trade" policy should consider the location of CO_2 emissions, as the underlying assumption of the policy is incorrect.

Although CO_2 is generally well-mixed in the atmosphere, data indicate that its mixing ratios are higher in urban than in background air, resulting in *urban CO_2 domes*[1-5]. Measurements in Phoenix, for example, indicate that peak and mean CO_2 in the city center are 75% and 38-43% higher, respectively, than in surrounding rural areas[2]. Many recent studies have examined the impact of global greenhouse gases on air pollution[7-14]. However, no study has isolated the impact of locally-emitted CO_2 on local air pollution, health, or climate. If locally-emitted CO_2 increases local air

pollution, then cities, counties, states, and small countries can reduce air pollution health problems by reducing their own CO_2 emissions, regardless of whether other air pollutants are reduced locally or whether other locations reduce CO_2.

For this study, the nested global-through-urban 3-D model, GATOR-GCMOM[15-20] was use to examine the effects of locally-emitted CO_2 on local climate and air pollution on two scales, California as a whole and the Los Angeles basin. Three pairs of baseline and sensitivity simulations were run: one pair nested from the globe to California for one year and two pairs nested from the globe to California to Los Angeles, each for three months (Aug-Oct; Feb-Apr). In each sensitivity simulation, only anthropogenic CO_2 emissions ($emCO_2$) were removed from the finest domain. Initial ambient CO_2 was the same in all domains of both simulations and $emCO_2$ was the same in the parent domains of both. As such, all resulting differences were due solely to locally-emitted (in the finest domain) CO_2.

The model and comparisons with data have been described over 16 years, including recently[15-20]. Figure 1 further compares modeled O_3, PM_{10}, and CH_3CHO from August 1-7 of the baseline (with $emCO_2$) and sensitivity (no $emCO_2$) simulations from the Los Angeles domain with data. The comparisons indicate very good agreement with respect to ozone in particular and that $emCO_2$ increased O_3, PM_{10}, and CH_3CHO almost immediately, during day and night.

Figure 2a shows the modeled contribution to surface CO_2 of California's CO_2 emissions. The CO_2 domes over Los Angeles, the San Francisco Bay Area, and parts of the Central Valley are evident. The largest CO_2 increase (5%, or 17.5 ppmv) was lower than observed increases in cities (*1*) since the resolution of the California domain was coarser than the resolution of measurements. As shown for Los Angeles shortly, an increase in model resolution increases the magnitude of the CO_2 dome. Whereas the population-weighted (PW) and domain-averaged (DA) increases in surface CO_2 due to $emCO_2$ were 7.4 ppmv and 1.3 ppmv, respectively, the corresponding increases in column CO_2 were 6.0 g/m^2 and 1.53 g/m^2, respectively, indicating that changes in column CO_2 were spread horizontally more than were changes in surface CO_2. This is because local $emCO_2$ starts mixing with

the larger scale soon after emissions, but the losses are quickly replaced with more local CO_2 emissions.

The CO_2 increases in California increased the PW air temperature by about 0.0063 K, more than it changed the domain-averaged air temperature (+0.00046) (Fig. 2b). Thus, CO_2 domes had greater temperature impacts where the CO_2 was emitted and where people lived than they had in the domain average. This result holds for the effects of emCO_2 on column water vapor (Fig. 2c - PW: +4.3 g/m^2; DA: +0.88 g/m^2), ozone (Fig. 2d – PW: +0.06 ppbv; DA: +0.0043 ppbv), $PM_{2.5}$ (Fig. 2f – PW: +0.08 μg/m^3; DA: -0.0052 μg/m^3), PAN (Fig. 2h – PW: +0.002 ppbv; DA: -0.000005 ppbv) and particle nitrate (Fig. 2i – PW: +0.030 μg/m^3; DA: +0.00084 μg/m^3).

Figure 3 elucidates correlations between changes in local ambient CO_2 caused by emCO_2 and changes in other parameters. Modeled temperature, water vapor, ozone, and $PM_{2.5}$ increased more in grid cells with larger ambient CO_2 increases than in cells with smaller ambient CO_2 increases. In other words, increases in ozone and $PM_{2.5}$ correlated spatially with local CO_2 increases. Figure 2 shows further that ozone increases correlated spatially with temperature and water vapor increases, both of which increase ozone particularly at high ozone[15].

$PM_{2.5}$ correlated slightly negatively (R=0.017) with higher temperature but more strongly positively (R=0.23) with higher water vapor (Fig. 2). Higher temperature decreased $PM_{2.5}$ by increasing vapor pressures thus PM evaporation and by enhancing precipitation in some locations. Some $PM_{2.5}$ decreases from higher temperatures were offset by biogenic organic emission increases from higher temperatures followed by biogenic oxidation to organic PM. But in California, biogenic emissions are lower than in the southeast U.S. Some $PM_{2.5}$ decreases were also offset by slower winds caused by enhanced boundary-layer stability from CO_2. While higher temperatures slightly decreased $PM_{2.5}$, higher water vapor due to emCO_2 increased $PM_{2.5}$ by increasing aerosol water content, increasing nitric acid and ammonia gas dissolution, forming more particle nitrate (Fig. 2i) and ammonium. Higher ozone from higher water vapor also increased oxidation of organic gases to organic PM. Since $PM_{2.5}$ increased overall due to emCO_2, water vapor increases of PM exceeded temperature decreases.

Health effect rates (y) due to pollutants in each model domain were determined from

$$y = y_0 \sum_i \left\{ P_i \sum_t \left(1 - \exp\left[-\beta \times \max\left(x_{i,t} - x_{th}, 0 \right) \right] \right) \right\} \quad (1)$$

where $x_{i,t}$ is the concentration in grid cell i at time t, x_{th} is the threshold concentration below which no health effect occurs, β is the fractional increase in risk per unit x, y_0 is the baseline health effect rate, and P_i is the grid cell population. Table 1 provides sums or values of P , β, y_0, and x_{th}.

California's local CO_2 resulted in ~13 (6-19) additional ozone-related deaths/year (Fig. 2e), or 0.3% above the baseline 4600 (2300-6900) deaths/year (Table 1). Higher $PM_{2.5}$ due to emCO_2 contributed another ~39 (13-60) deaths/year (Fig. 2g), 0.2% above the baseline death rate of 22,500 (5900-42,000) deaths/year. Changes in cancer due to emCO_2 were relatively small (Table 1).

Simulations for Los Angeles echo results for California but allowed for a higher-resolution, more accurate picture of the effects of emCO_2. Figure 4 (Feb-Apr) indicates that the CO_2 dome that formed over Los Angeles peaked at about 34 ppmv, twice that over the coarser California domain. The column difference indicates a spreading of the dome over a larger area than the surface dome. In Feb-Apr and Aug-Oct, emCO_2 enhanced PW ozone and $PM_{2.5}$, increasing mortality (Fig. 4, Table 1) and other health effects (Table 1). The causes of such increases, however, differed with season. From Feb-Apr, emCO_2 increased surface temperatures and water vapor over the Los Angeles basin (Fig. 4). This slightly enhanced ozone and $PM_{2.5}$, but the increase in the land-ocean temperature gradient also increased sea-breeze wind speeds, increasing resuspension of road and soil dust and moving particulate matter more to the eastern basin. From Aug-Oct, emCO_2 increased temperatures aloft, increasing the land-sea temperature gradient and wind speed aloft, increasing the flow of moisture from the ocean to land aloft, increasing water vapor and clouds over land, decreasing surface solar radiation, causing a net decrease in local ground temperatures and UV radiation but a net increase in water vapor at all altitudes due to the vertical diffusion of water vapor aloft to the surface. The higher water vapor triggered higher ozone and relative humidities, which increased

aerosol particle swelling, increasing gas growth onto aerosols, and reducing particle evaporation. In sum, emCO_2 increased ozone and $PM_{2.5}$ and their corresponding health effects in both seasons, increasing air pollution deaths in California and Los Angeles by about 50-100 per year (Fig. 4, Table 1). Death rates for Los Angeles were similar or higher than those for California due to the greater accuracy of higher resolution (Los Angeles) simulations, as shown in Table 2 of Ref 17; thus, these results are likely to be conservative for California as a whole.

The California mortality increase compares with a U.S. death rate increase of about 1000/yr per 1 K rise due to all globally-emitted anthropogenic CO_2, with about 300 deaths/yr occurring in California[15], which has 12% of the U.S. population. The greater death rates in California versus the rest of the U.S. are due to the fact that higher temperatures and water vapor due to CO_2 enhance air pollution the most where it is already high, and California has 6 of the top 10 polluted cities in the U.S.

Worldwide, emissions of many pollutants (e.g., NO_x, HCs, CO, PM) that cause local air pollution are regulated. The few CO_2 emission regulations proposed to date have been justified based on the large-scale climate effects and resulting feedbacks to sea levels, water supply, and global air pollution that such emissions cause. However, no proposed CO_2 regulation is based on the potential impact of locally-emitted CO_2 on local pollution as such effects have been assumed not to exist[6]. The result here suggests that reducing local CO_2 will reduce 50-100 California air pollution deaths/yr even if CO_2 in adjacent regions is not controlled. Thus, CO_2 emission controls are justified on the same grounds that NO_x, HC, CO, and PM emission regulations are justified. Results further imply that the assumption behind the "cap and trade" policy, namely that CO_2 emitted in one location has the same impact as CO_2 emitted in another, is incorrect, as CO_2 emissions in populated cities have larger health impacts than CO_2 emissions in unpopulated areas. As such, CO_2 cap and trade, if done, should consider the location of emissions to avoid additional health damage.

References

1. Idso, C.D., Idso, S.B. & Balling Jr. R.C. The urban CO_2 dome of Phoenix, Arizona. *Physical Geography* **19**, 95-108 (1998).

2. Idso, C.D., Idso, S.B. & Balling Jr., R.C. An intensive two-week study of an urban CO2 dome in Phoenix, Arizona, USA. *Atmos. Environ.* **35**, 995-1000 (2001).

3. Gratani, L. & Varone, L. Daily and seasonal variation of CO_2 in the city of Rome in relationship with the traffic volume. *Atmos. Environ.* **39**, 2619-2624 (2005).

4. Newman, S., Xu, X., Affek, H.P., Stolper, E., & Epstein, S. Changes in mixing ratio and isotopic composition of CO2 in urban air from the Los Angeles basin, California, between 1972 and 2003. *J. Geophys. Res.* **113**, D23304, doi:10.1029/2008JD009999 (2008).

5. Rigby, M., Toumi, R., Fisher, R. Lowry, D. & Nisbet, E.G. First continuous measurements of CO2 mixing ratio in central London using a compact diffusion probe. *Atmos. Environ.* **42**, 8943-8953 (2008).

6. Johnson, S.L California State Motor Vehicle Pollution Control Standards; Notice of Decision Denying a Waiver of Clean Air Act Preemption for California's 2009 and Subsequent Model Year Greenhouse Gas Emission Standards for New Motor Vehicles. *Federal Register* **73** (45), 12,156-12,169 (2008).

7. Knowlton, K., Rosenthal, J.E., Hogrefe, C., Lynn, B., Gaffin, S., Goldberg, R., Rosenzweig, C., Civerolo, K., Ku, J.-Y. & Kinney P.L. Assessing ozone-related health impacts under a changing climate. *Environ. Health Perspectives* **112**, 1557-1563 (2004).

8. Mickley, L.J., Jacob, D.J., Field, B.D. & Rind, D. Effects of future climate change on regional air pollution episodes in the United States. *Geophys. Res. Lett.* **31**, L24103, doi:10.1029/2004GL021216 (2004).

9. Stevenson, D., Doherty, R., Sanderson, M., Johnson, C., Collins, B. & Derwent, D. Impacts of climate change and variability on tropospheric ozone and its precursors. *Faraday Disc.* **130**, 1-17 (2005).

10. Brasseur, G.P., Schultz, M.M., Granier, C., Saunois, M., Diehl, T., Botzet, M. & Roeckner E. Impact of climate change on the future chemical composition of the global troposphere. *J. Clim.* **19**, 3932-3951 (2006).

11. Steiner, A.L., Tonse, S., Cohen, R.C., Goldstein, A.H. & Harley R.A. Influence of future climate and emissions on regional air quality in California. *J. Geophys. Res.* **111**, D18303, doi:10.1029/2005JD006935 (2006).

12. Unger, N., Shindell, D.T., Koch, D.M., Ammann, M., Cofala, J. & Streets D.G. Influences of man-made emissions and climate changes on tropospheric ozone, methane, and sulfate at 2030 from a broad range of possible futures. *J. Geophys. Res.* **111**, D12313, doi:10.1029/2005JD006518 (2006).

13. Liao, H., Chen, W.-T. & Seinfeld J.H. Role of climate change in global predictions of future tropospheric ozone and aerosols. *J. Geophys. Res.* **111**, D12304, doi:10.1029/2005JD006852 (2006).

14. Bell, M.L., Goldberg, R., Hogrefe, C., Kinney, P.L., Knowlton, K., Lynn, B., Rosenthal J., Rosenzweig, C. & Patz, J.A. Climate change, ambient ozone, and health in 50 U.S. cities. *Climatic Change* **82**, 61-76 (2007).

15. Jacobson, M.Z. On the causal link between carbon dioxide and air pollution mortality. *Geophys. Res. Lett.* **35**, L03809, doi:10.1029/2007GL031101 (2008).

16. Jacobson, M.Z. & Streets D.G. The influence of future anthropogenic emissions on climate, natural emissions, and air quality. *J. Geophys. Res.*, in press (2009).

17. Jacobson, M.Z. GATOR-GCMM: 2. A study of day- and nighttime ozone layers aloft, ozone in national parks, and weather during the SARMAP Field Campaign. *J. Geophys. Res.* **106**, 5403-5420 (2001).

18. Jacobson, M.Z., Kaufmann, Y.J. & Rudich, Y. Examining feedbacks of aerosols to urban climate with a model that treats 3-D clouds with aerosol inclusions. *J. Geophys. Res.* **112**, doi:10.1029/2007JD008922 (2007).

19. Jacobson, M.Z. Effects of wind-powered hydrogen fuel cell vehicles on stratospheric ozone and global climate. *Geophys. Res. Lett.* **35**, L19803, doi:10.1029/2008GL035102 (2008).

20. Jacobson, M.Z. The short-term effects of agriculture on air pollution and climate in California. *J. Geophys. Res.* **113**, D23101, doi:10.1029/2008JD010689 (2008).

21. United States Environmental Protection Agency (USEPA), AIR Data, http://www.epa.gov/air/data/ (2006).

22. Thurston, G.D. & Ito K. Epidemiological studies of acute ozone exposures and mortality. *J. Exposure Analysis and Env. Epidemiology* **11**, 286-294 (2001).

23. Hoyert, D.L., Heron, M.P., Murphy, S.L. & Kung H.-C. National Vital Statistics Reports, Vol. 54, No. 13, http://www.cdc.gov/nchs/fastats/deaths.htm (2006).

24. Merrill, C.T. & Elixhauser, A. HCUP Fact Book No. 6: Hospitalization in the United States, 2002. Appendix, www.ahrq.gov/data/hcup/factbk6/factbk6e.htm (2005).

25. Mannino, D.M., Homa, D.M., Akinbami, L.J., Moorman, J.E., Gwynn, C. & Redd S.C. Center for Disease Control Morbidity and Mortality Weekly Report. *Surveillance Summaries* **51** (SS01), 1-13 (2002).

26. Ostro, B.D., Tran, H. & Levy, J.I. The health benefits of reduced tropospheric ozone in California. *J. Air & Waste Manage. Assoc.* **56**, 1007-1021 (2006).

27. Pope III, C.A., Burnett, R.T., Thun, M.J., Calle, E.E., Krewski, D., Ito, K., Thurston, G.D. Lung cancer, cardiopulmonary mortality, and long-term exposure to fine particulate air pollution. *JAMA,* **287**, 1132-1141 (2002).

Acknowledgements

Support came from the U.S. Environmental Protection Agency grant RD-83337101-O, NASA grant NX07AN25G, and the NASA High-End Computing Program.

Figure Captions

Figure 1. (a) Paired-in-time-and-space comparisons of modeled baseline (solid lines), modeled no-emCO_2 (dashed lines), and data[21] (dots) for ozone, sub-10-μm particle mass, and acetaldehyde from the Los Angeles domain for August 1-7, 2006. The resolutions of the global, California, and Los Angeles domains were 4° SN x 5° WE, 0.20° SN x 0.15° WE, and 0.45° SN x 0.05° WE, respectively. The global domain included 47 sigma-pressure layers up to 0.22 hPa (≈60 km), with very high resolution (15 layers) in the bottom 1 km. The nested regional domains included 35 layers exactly matching the global layers up to 65 hPa (≈18 km). The model was run without data assimilation or model spinup.

Figure 2. Modeled annually averaged difference for several surface or column parameters when two simulations (with and without emCO_2) were run. The numbers in parentheses are population-weighted changes.

Figure 3. Scatter plots of paired-in-space one-year-averaged changes between several parameter pairs, obtained from all near-surface grid cells of the California domain. Also shown is an equation for the linear fit through the data points in each case.

Figure 4. Same as Fig. 2., but for the Los Angeles domain and for Feb-Apr and Aug-Oct. Also shown are scatter plots for Aug-Oct similar to those for Fig. 3.

Table 1. Summary of locally-emitted CO_2's ($emCO_2$) effects on cancer, ozone mortality, ozone hospitalization, ozone emergency-room (ER) visits, and particulate-matter mortality in California. Results are shown for the with-$emCO_2$ emissions simulation ("Base") and the difference between the base and no $emCO_2$ emissions simulations ("Base minus no-$emCO_2$") for California and Los Angeles. The domain summed populations in the Los Angeles and California domains were 17.268 million and 35.35 million, respectively. All concentrations are near-surface values weighted spatially by population. Los Angeles results were an average of Feb-Apr and Aug-Oct results.

	Annual base Calif.	Base minus no $emCO_2$ Calif.	Annual Base LA	Base minus no $emCO_2$ LA
Ozone ≥ 35 ppbv (ppbv)	47.4	+0.060	44.7	+0.12
$PM_{2.5}$ ($\mu g/m^3$)	50.0	+0.08	36	+0.29
Formaldehyde (ppbv)	4.43	+0.0030	4.1	+0.054
Acetaldehyde (ppbv)	1.35	+0.0017	1.3	+0.021
1,3-Butadiene (ppbv)	0.11	-0.00024	0.23	+0.0020
Benzene (ppbv)	0.30	-0.00009	0.37	+0.0041
Cancer				
USEPA cancers/yr+	44.1	0.016	22.0	+0.28
OEHHA cancers/yr+	54.4	-0.038	37.8	+0.39
Ozone health effects				
High O_3 deaths/yr*	6860	+19	2140	+20
Med. O_3 deaths/yr*	4600	+13	1430	+14
Low O_3 deaths/yr*	2300	+6	718	+7
O_3 hospitalizations/yr*	26,300	+65	8270	+75
Ozone ER visits/yr*	23,200	+56	7320	+66
PM health effects				
High $PM_{2.5}$ deaths/yr^	42,000	+60	16,220	+147
Medium $PM_{2.5}$ deaths/yr^	22,500	+39	8500	+81
Low $PM_{2.5}$ deaths/yr^	5900	+13	2200	+22

(+) USEPA and OEHHA cancers/yr were found by summing, over all model surface grid cells and the four carcinogens (formaldehyde, acetaldehyde, 1,3-butadiene, and benzene), the product of individual CUREs (cancer unit risk estimates=increased 70-year cancer risk per $\mu g/m^3$ sustained concentration change), the mass concentration ($\mu g/m^3$) (for baseline statistics) or mass concentration difference (for difference statistics) of the carcinogen, and the population in the cell, then dividing by the population of the model domain and by 70 yr. USEPA CURES are $1.3x10^{-5}$ (formaldehyde), $2.2x10^{-6}$ (acetaldehyde), $3.0x10^{-5}$ (butadiene), $5.0x10^{-6}$ (=average of $2.2x10^{-6}$ and $7.8x10^{-6}$) (benzene) (www.epa.gov/IRIS/). OEHHA CUREs are $6.0x10^{-6}$ (formaldehyde), $2.7x10^{-6}$ (acetaldehyde), $1.7x10^{-4}$ (butadiene), $2.9x10^{-5}$ (benzene) (www.oehha.ca.gov/risk/ChemicalDB/index.asp).

(*) High, medium, and low deaths/yr, hospitalizations/yr, and emergency-room (ER) visits/yr due to short-term O_3 exposure were obtained from Equation 1, assuming a threshold of 35 ppbv[22]. The baseline 2003 U.S. death rate (y_0) was 833 deaths/yr per 100,000[23]. The baseline 2002 hospitalization rate due to respiratory problems was 1189 per 100,000[24]. The baseline 1999 all-age emergency-room visit rate for asthma was 732 per 100,000[25]. The fractional increases (β) in the number of deaths from all causes due to ozone were 0.006, 0.004, and 0.002 per 10 ppbv increase in daily 1-hr maximum ozone[26]. These were multiplied by 1.33 to convert the risk associated with a 10 ppbv increase in 1-hr maximum O_3 to that associated with a 10 ppbv increase in 8-hour average O_3[22]. The central value of the increased risk of hospitalization due to respiratory disease was 1.65% per 10 ppbv increase in 1-hour maximum O_3 (2.19% per 10 ppbv increase in 8-hour average O_3), and that for all-age ER visits for asthma was 2.4% per 10 ppbv increase in 1-hour O_3 (3.2% per 10 ppbv increase in 8-hour O_3)[24,25].

(^) The death rate due to long-term $PM_{2.5}$ exposure was calculated from Equation 1. Increased death risks to those ≥30 years were 0.008 (high), 0.004 (medium), and 0.001 (low) per 1 $\mu g/m^3$ $PM_{2.5}$ >8 $\mu g/m^3$ based on 1979-1983 data[27]. From 0-8 $\mu g/m^3$, the increased risks here were assumed =¼ those >8 $\mu g/m^3$ to account for reduced risk near zero $PM_{2.5}$[15]. The all-cause 2003 U.S. death rate of those ≥30 years was 809.7 deaths/yr per 100,000 total population.

Figure 1

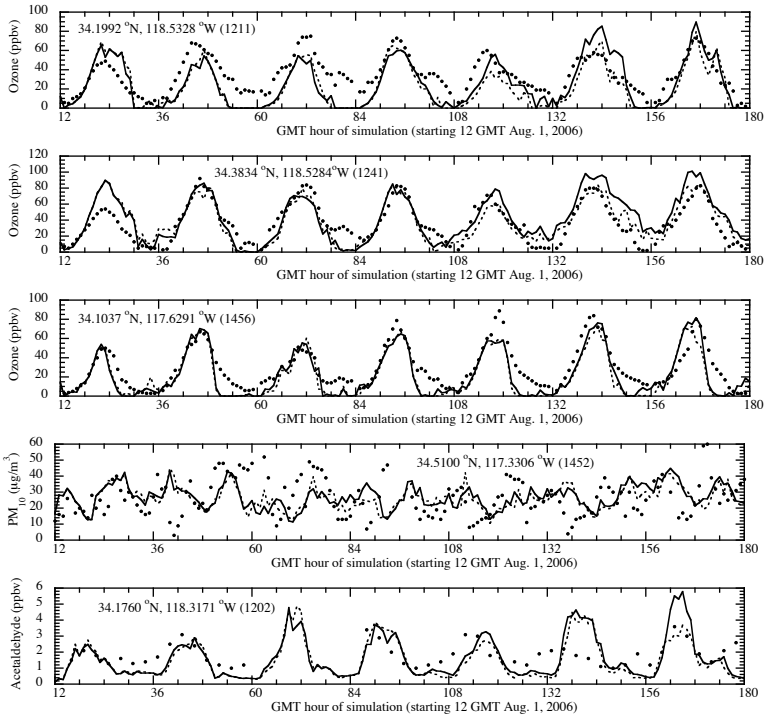
34.1992 °N, 118.5328 °W (1211)
Ozone (ppbv)
34.3834 °N, 118.5284°W (1241)
Ozone (ppbv)
34.1037 °N, 117.6291 °W (1456)
Ozone (ppbv)
34.5100 °N, 117.3306 °W (1452)
PM10 (μg/m3)
34.1760 °N, 118.3171 °W (1202)
Acetaldehyde (ppbv)
GMT hour of simulation (starting 12 GMT Aug. 1, 2006)

Figure 2

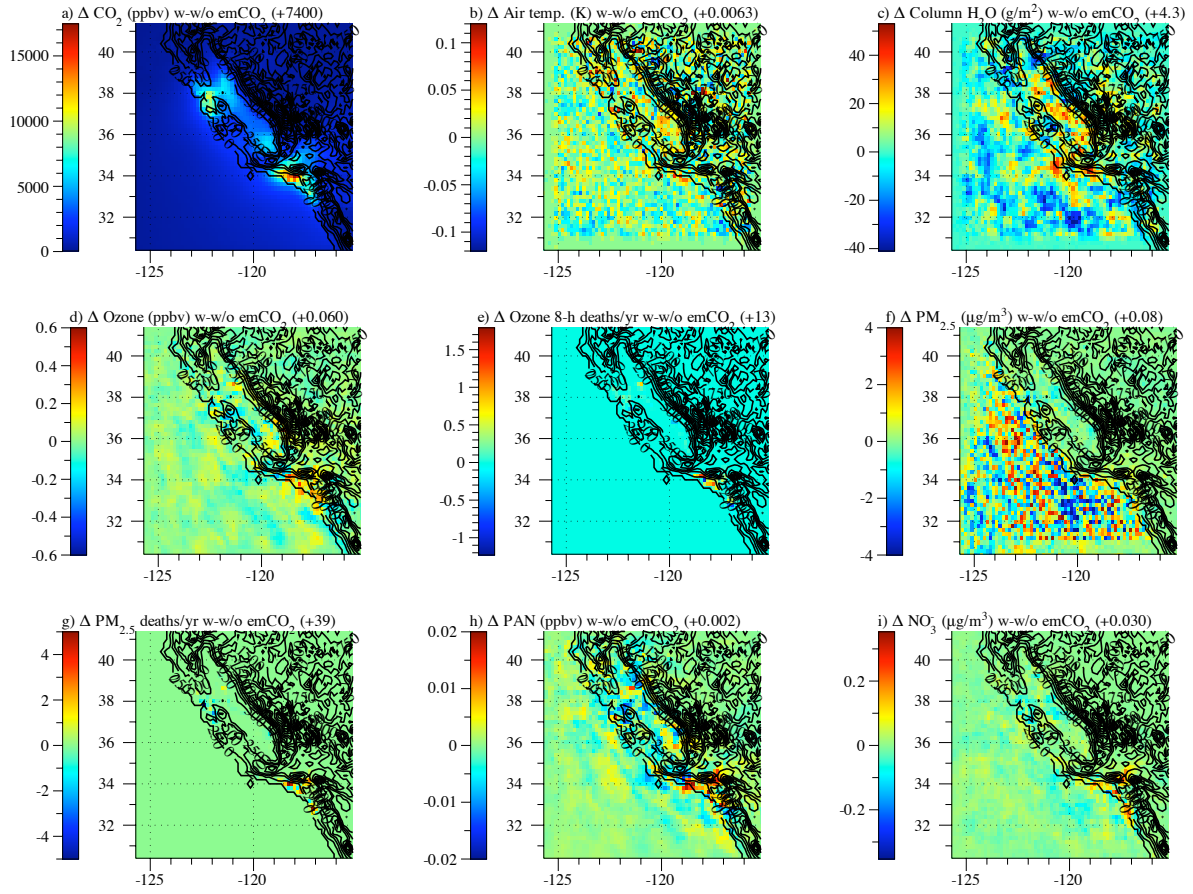
a) Δ CO2 (ppbv) w-w/o emCO2 (+7400)
b) Δ Air temp. (K) w-w/o emCO2 (+0.0063)
c) Δ Column H2O (g/m2) w-w/o emCO2 (+4.3)
d) Δ Ozone (ppbv) w-w/o emCO2 (+0.060)
e) Δ Ozone 8-h deaths/yr w-w/o emCO2 (+13)
f) Δ PM2.5 (µg/m3) w-w/o emCO2 (+0.08)
g) Δ PM2.5 deaths/yr w-w/o emCO2 (+39)
h) Δ PAN (ppbv) w-w/o emCO2 (+0.002)
i) Δ NO3- (µg/m3) w-w/o emCO2 (+0.030)

Figure 3

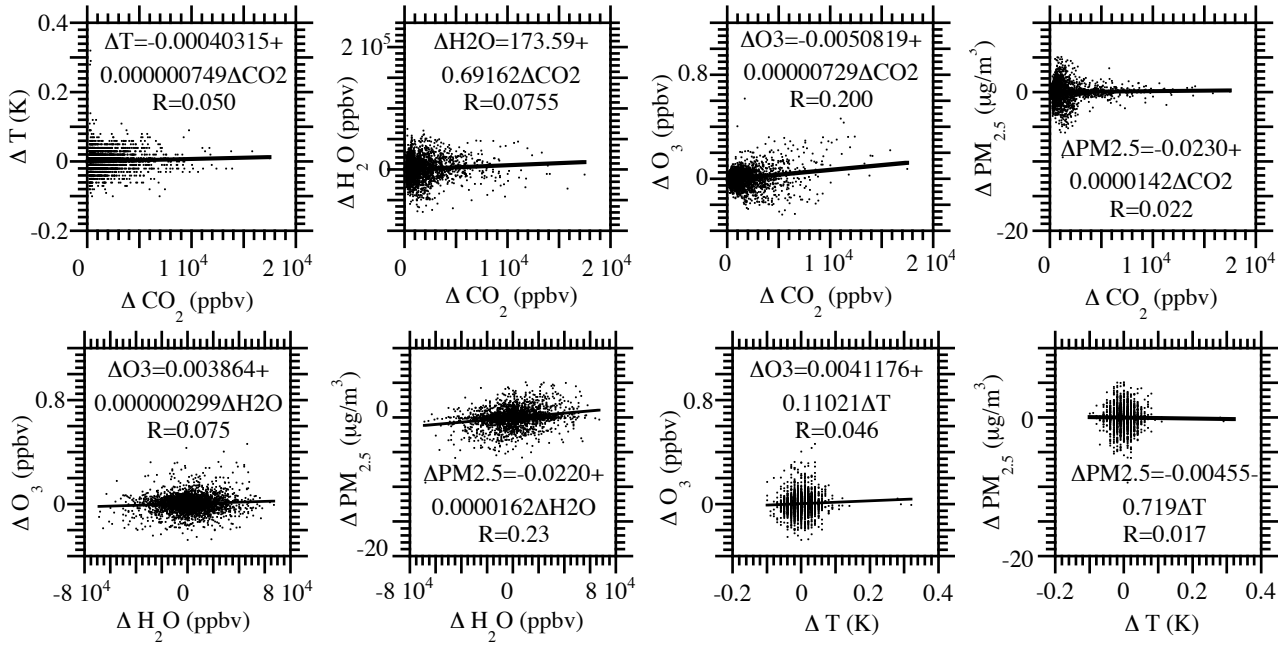
ΔT=-0.00040315+
0.000000749ΔCO2
R=0.050
ΔT (K)
ΔCO2 (ppbv)
ΔH2O=173.59+
0.69162ΔCO2
R=0.0755
ΔH2O (ppbv)
ΔCO2 (ppbv)
ΔO3=-0.0050819+
0.00000729ΔCO2
R=0.200
ΔO3 (ppbv)
ΔCO2 (ppbv)
ΔPM2.5=-0.0230+
0.0000142ΔCO2
R=0.022
ΔPM2.5 (μg/m3)
ΔCO2 (ppbv)
ΔO3=0.003864+
0.000000299ΔH2O
R=0.075
ΔO3 (ppbv)
ΔH2O (ppbv)
ΔPM2.5=-0.0220+
0.0000162ΔH2O
R=0.23
ΔPM2.5 (μg/m3)
ΔH2O (ppbv)
ΔO3=0.0041176+
0.11021ΔT
R=0.046
ΔO3 (ppbv)
ΔT (K)
ΔPM2.5=-0.00455-
0.719ΔT
R=0.017
ΔPM2.5 (μg/m3)
ΔT (K)

Figure 4

February-April

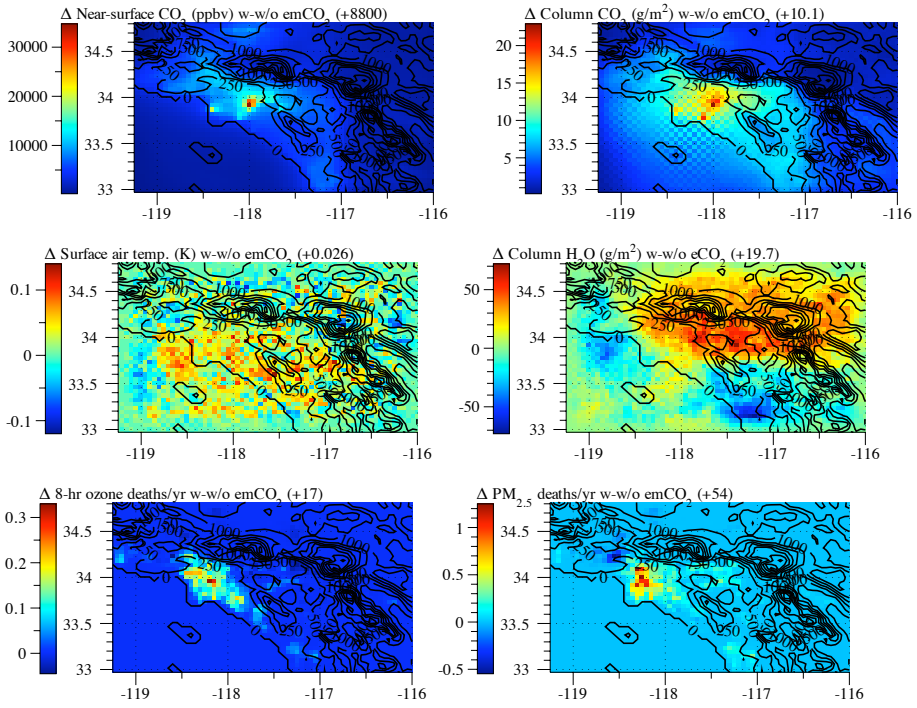

August-October